Chapter 3: Kinematic Position Analysis

Kinematic position analysis is the first step in creating a complete mathematical model of the new manipulator architecture. This analysis will begin by developing a general descriptive model that characterizes the kinematic geometry of the device. From this geometric model, a mathematical function relating the input-to-output position parameters will be formed. The goal of this function is to describe the forward and inverse position relationships in closed-form. The position analysis will also be demonstrated when the wrist is kinematically constrained to behave as a spherical two degree-of-freedom orienting device. Finally, the kinematic position solutions will be used to generate kinematic workspace plots that demonstrate the manipulator's range of motion.

3.1 Review of Similar Geometric Architectures

The first reference to a geometry similar to that of the proposed wrist was by Clemens, (1872) who patented a parallel chain R-R-S-R-R spatial linkage that formed a constant velocity coupling. In 1973, Hunt cataloged a variety of couplings, including this R-R-S-R-R coupling. Although these devices have an architecture similar to that of the proposed wrist, they differ substantially in application. For example, all of these earlier works treat the device as a passive torque coupling rather than as an actuated positioning device. This research has evolved from the shaft coupling research and the author's work with parallel robotic platform manipulators and an all-revolute constant-velocity coupling (Salerno, 1994), (Canfield and Reinholtz, 1995), (Canfield et al., 1994). All the devices share a common basic geometric architecture, called the double octahedron, shown in Fig. 3.1.

3.2 Geometric Model of the Wrist Architecture

A schematic diagram illustrating the geometry of the Carpal wrist is shown in Fig. 3.2. This wrist consists of two rigid plates, referred to as the basal and distal plates, coupled together by three five-revolute (RRRRR) chains, with the central three revolutes intersecting at a common point. As a simplification, the central three intersecting revolutes could be replace with a spheric joint. However, it is considered that this all-revolute design will lead to increased reliability and superior precision. Although other possible geometries exist, this paper will specifically address configurations in which the revolute axes of the basal and distal plates form equilateral triangles with base dimension, *b,* and which have six connecting arms of equal length, *l.* This symmetric construction was specifically chosen to result in a closed-form kinematic analysis. By actuating the three basal revolute joints, $\theta_1,$ $\theta_2,$ and $\theta_3,$ the motion of the distal plate may be controlled relative to the basal plate. This wrist is capable of producing pitch and yaw rotations in excess of 180 degrees combined with a third translational or "plunging" motion. The plunging motion is defined as an extension along the normal axis of the distal plate. A fourth degree-of-freedom may be added in the form of a revolute joint on the distal plate that allows rotation about the pointing direction to accommodate tasks requiring general orientations of the end-effector. Note

that adding roll motion in this manner results in an overall structure that is no longer parallel, but rather a hybrid parallel/serial device. Issues involved with adding a roll degree of freedom to the Carpal Wrist are addressed in detail in Chap. 7.
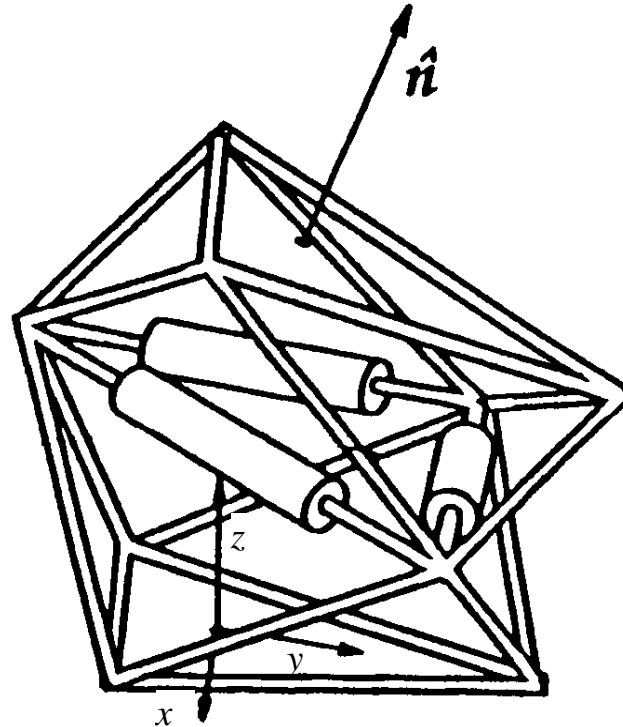
Figure 3.1: Schematic of Double Octahedron

The plunging motion of the proposed wrist potentially creates control challenges. This degree-of-freedom complicates the solution to the inverse kinematics of the manipulator since the plunge capability creates a redundant positioning problem. In some applications the extra degree-of-freedom may be advantageous; for example in increasing manipulator dexterity or increasing available workspace. However, for many industrial applications it is an unnecessary redundant degree of freedom. One way of resolving this control problem is by coupling the three degrees-of-freedom (pitch, yaw, and plunge) such that the wrist is only capable of producing pitch and yaw orientation. The constraint on the plunge motion may be imposed by coupling the control of the actuators through the control algorithms, as demonstrated in this chapter, or by physically coupling the device such that only the two angular motions may occur. Operated in this two degree-of-freedom mode, the device is a true spherical wrist, and the manipulator/wrist combination will satisfy necessary criteria for a closed-form solution of a six degree-of-freedom manipulator, e.g., Pieper's criteria (Craig, 1989).

3.3 Kinematic Position Analysis of Proposed Wrist Architecture

This section will develop closed-form solutions to both the forward and inverse kinematic analyses of the proposed wrist. Spherical constraints will then be developed and imposed on the inverse kinematic solution. Finally, this solution will be used to develop workspace plots.

From the kinematic diagram shown in Fig. 3.2, the geometry of the basal and distal plates can be characterized by the location and orientation of their corresponding revolute joints. These revolutes were chosen to lie on equilateral triangles with the center of each revolute located at the midpoint of each side of the triangle and the axes of the revolutes coincident with the sides of the triangle. The revolutes of the basal and distal plates are located by vectors $\mathbf{b}_i$ and $\mathbf{d}_i$ ($i = 1...3$), respectively. The orientation of each basal revolute are denoted by the unit vectors $\hat{\mathbf{u}}_i$ ($i = 1...3$). The midpoint of each branch is the point of intersection for the center three revolutes and are labeled as points $\mathbf{m}_i$ ($i = 1...3$). Also shown in Fig. 3.2 is the mid-plane of the wrist which is defined by the midpoints of the three branches. This midplane forms a plane of symmetry for this particular wrist geometry. Coordinate frames **{B}** and **{D}** are located at the centroids of the basal and distal plates with the *z*-axis of each coordinate frame normal to its corresponding plate and with each corresponding *x*-axis pointing toward the first nodal point, $\mathbf{b}_1$ or $\mathbf{d}_1$ (see Figs. 3.2 and 3.3). The centroid of the basal plate, $\mathbf{c}_B$, is the system origin. The geometric center of the wrist, $\mathbf{c}_W$ is defined as the intersection of the normal-axes of the basal and distal coordinate frames. This position is unique in that the distance from $\mathbf{c}_W$ to either $\mathbf{c}_D$ or $\mathbf{c}_B$ is equal to the plunge distance, p_d. While the geometric center does not necessarily lie on any physical part of
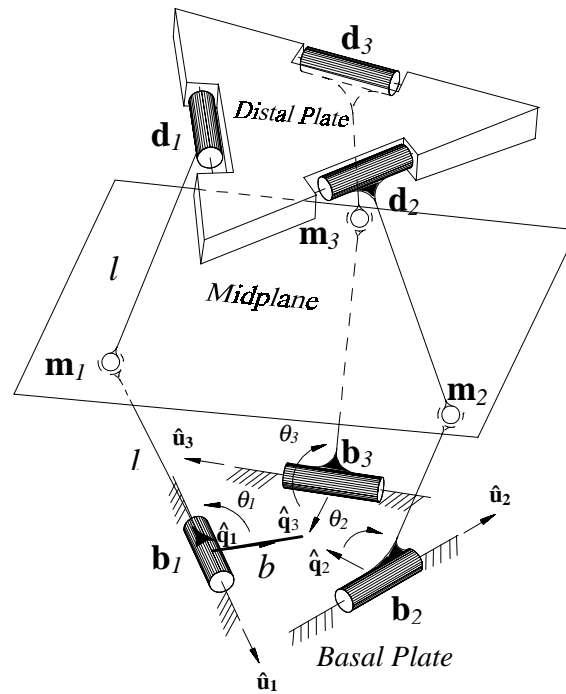

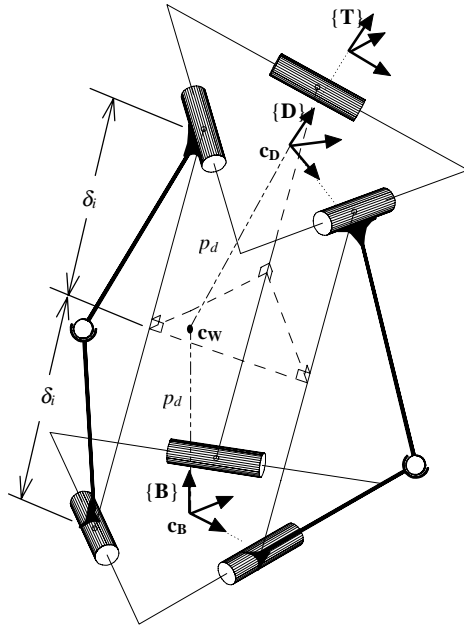**Figure 3.2: Kinematic Diagram of Proposed Wrist**

Figure 3.3: Wrist Reference Frames

the wrist, it is important because, in the spherically constrained mode, the motion of the distal coordinate frame describes a sphere of radius p_d about the geometric center of the wrist. The final roll axis, when included, is configured such that the tool coordinate frame {**T**} rotates about the *z*-axis of frame {**D**}.

3.3.1 Forward Kinematic Analysis

The forward kinematic problem for this manipulator can be stated as: *given a set of basal revolute angles (θ_1, θ_2, θ_3), and a roll angle, (θ_r), find the position and orientation of the tool coordinate frame.*

With the location of the basal revolutes and their corresponding angles known, the location of the mid-points of each branch are found as follows:

$$\mathbf{m}_i = \mathbf{R}_{[\hat{\mathbf{u}}_i,\theta_i]} l\hat{\mathbf{q}}_i + \mathbf{b}_i \qquad i = 1\cdots 3 \tag{3.1}$$

where $\mathbf{R}_{[\hat{\mathbf{u}}_i,\theta_i]}$ represents a rotation about axis $\hat{\mathbf{u}}_i$ by an amount θ_i, and $\hat{\mathbf{q}}_i$ defines an inward pointing unit vector perpendicular to $\hat{\mathbf{u}}_i$ lying in the base plane, as shown in Fig. 3.2.

Using the mid-points $\mathbf{m}_1$, $\mathbf{m}_2$, and $\mathbf{m}_3$, the plane coefficients, A_m, B_m, C_m, D_m, of the midplane can be determined in standard form as:

$$[A_m, B_m, C_m]^T = (\mathbf{m}_2 - \mathbf{m}_1) \times (\mathbf{m}_3 - \mathbf{m}_2) \tag{3.2}$$

Now that the midplane is defined, the perpendicular distance from each point, $\mathbf{b}_1$, $\mathbf{b}_2$, and $\mathbf{b}_3$, to the midplane can be found as follows:

$$\delta_i = \hat{\mathbf{N}}_m \cdot (\mathbf{m}_i - \mathbf{b}_i) \qquad i = 1 \cdots 3 \tag{3.3}$$

where the midplane normal, $\hat{\mathbf{N}}_m$, is defined as:

$$\hat{\mathbf{N}}_m = \frac{[A_m, B_m, C_m]^T}{\sqrt{A_m^2 + B_m^2 + C_m^2}} \tag{3.4}$$

Using the inherent midplane symmetry of the wrist shown in Fig. 3.3, the distal revolute centers may be located relative to the basal revolutes by traversing a distance $2(\delta_i)$ from each basal revolute in the direction of the midplane normal. Hence,

$$\mathbf{d}_i = \mathbf{b}_i + 2\delta_i \hat{\mathbf{N}}_m \qquad i = 1 \cdots 3 \tag{3.5}$$

These distal revolute centers define the distal plane. The position of the origin of the distal and tool coordinate frames, $\mathbf{c}_D$ and $\mathbf{c}_T$, are simply determined from the average or center position of the three distal revolutes.

$$\mathbf{c}_D = \mathbf{c}_T = (\mathbf{d}_1 + \mathbf{d}_2 + \mathbf{d}_3)/3 \tag{3.6}$$

The *z*-axis of the distal frame is identified from the vector cross-product.

$$\hat{\mathbf{z}}_D = \frac{(\mathbf{d}_2 - \mathbf{d}_1) \times (\mathbf{d}_3 - \mathbf{d}_2)}{|(\mathbf{d}_2 - \mathbf{d}_1) \times (\mathbf{d}_3 - \mathbf{d}_2)|} \tag{3.7}$$

The other axes of the distal coordinate frame may similarly be defined based on knowledge of the distal revolute positions:

$$\hat{\mathbf{x}}_D = \frac{\mathbf{d}_1 - \mathbf{c}_T}{|\mathbf{d}_1 - \mathbf{c}_T|} \tag{3.8}$$

$$\hat{\mathbf{y}}_D = -\hat{\mathbf{x}}_D \times \hat{\mathbf{z}}_D \tag{3.9}$$

Now that all axes of the distal frame are defined with respect to the basal frame, a rotation matrix characterizing the relative rotation between {$\mathbf{B}$} and {$\mathbf{D}$} may be expressed as:

$$_D^B\mathbf{R} = [\hat{\mathbf{x}}_D, \hat{\mathbf{y}}_D, \hat{\mathbf{z}}_D] \tag{3.10}$$

Note that this rotation matrix is a function of θ_1, θ_2, and θ_3. The last roll axis (when included) may now be accounted for as:

$$_T^B\mathbf{R} = {_D^B}\mathbf{R}\,\mathbf{R}_z(\theta_r) \tag{3.11}$$

where $_T^B\mathbf{R}$ is a rotation matrix that describes the orientation of the tool relative to the basal coordinate frame and $\mathbf{R}_z(\theta_r)$ is a rotation about the *z*-axis by an amount θ_r.

Now that the position and orientation of the tip frame are known with respect to the basal coordinate frame, it is possible to extract any description of rotation that best suits a particular application.

3.3.2 Inverse Kinematic Analysis

The inverse kinematic problem for the Carpal wrist architecture may be stated as: *given a desired end orientation and plunge distance, find a set of input angles, θ_1, θ_2, θ_3, that will produce this desired result*.

The inverse problem presents difficulties not present in the forward analysis. The primary complication results from the fact that only a two degree-of-freedom orientation can be achieved between the base and distal frames, {**B**} and {**D**}.

Briefly, the inverse kinematic solution for a specified position will proceed as follows:

1. Determine that the specified position and orientation lie within the three degree-of-freedom subspace of the wrist. That is to say, verify that the goal is attainable.

2. Use the given information to first position and orient the tool. This will simultaneously locate the center of the distal plate and determine its common normal.

3. From this resulting center position and common normal, the location of the distal revolutes may be uniquely determined.

4. With the location of the distal revolutes known, it is possible to solve for the required basal angles, θ_1 , θ_2 and θ_3.

5. When a roll axis is included, determine the relative rotation between the distal coordinate frame and the tool frame. This angle is the resulting roll axis angle, θ_r.

The first task above may be simplified by restricting the goal specification to a consistent set of three variables. For this wrist, it is natural to specify the pointing orientation (two parameters) and the plunge distance (one additional parameter). The architecture of the wrist prohibits relative rotation between the basal and distal plates about their common normal axes (Hunt, 1973), (Canfield and Reinholtz, 1993). This implies that only two angular degrees of freedom exist between the basal and distal plates. The pointing orientation of the tool may be specified using any convenient method. Ultimately, whatever description is used, it may be converted into a general rotation matrix.

To better visualize the inverse problem, the wrist will momentarily be modeled as two rods of length p_d (the plunge distance), joined by a spheric joint. Fig. 3.4 illustrates this model of the wrist. From the specified tool rotation matrix it is possible to extract the direction of the *z*-axis of the tool frame. This is simply the last column of the rotation matrix that describes the desired orientation. The components of this vector along with the components of the *z*-axis of the basal frame determine the axis of bending, $\hat{\mathbf{u}}_{bend}$, which is perpendicular to both. Continuing with the above model, the axis of bending is first defined, enabling the second link to be rotated about this

axis. The two orientational degrees-of-freedom are now given by the axis of bending and the angle, ϕ, which specifies the degree of bending.

Step two may be accomplished by evaluating $\hat{\mathbf{u}}_{bend}$ and ϕ:

$$\hat{\mathbf{u}}_{bend} = \frac{\hat{\mathbf{z}}_T \times \hat{\mathbf{z}}_B}{\left|\hat{\mathbf{z}}_T \times \hat{\mathbf{z}}_B\right|} \tag{3.12}$$

$$\phi = cos^{-1}\left(\hat{\mathbf{z}}_T \cdot \hat{\mathbf{z}}_B\right) \tag{3.13}$$

where, $\hat{\mathbf{z}}_B$, $\hat{\mathbf{z}}_T$ are the *z*-axes of the basal and tool frames respectively.

The location of the distal revolute joints may now be found by rotating their undeflected positions as follows:

$$\mathbf{d}_i = \mathbf{R}_{(\hat{\mathbf{u}}_{bend}, \phi_i)}\mathbf{d}'_i \qquad i = 1,....,3 \tag{3.14}$$

where

$$\mathbf{R}_{(\hat{\mathbf{u}}_{bend}, \phi)} = \begin{bmatrix} k_x k_x v\phi + c\phi & k_x k_y v\phi - k_z s\phi & k_x k_z v\phi + k_y s\phi \\ k_x k_y v\phi + k_z s\phi & k_y k_y v\phi + c\phi & k_y k_z v\phi - k_x s\phi \\ k_x k_z v\phi - k_y s\phi & k_y k_z v\phi + k_x s\phi & k_z k_z v\phi + c\phi \end{bmatrix}, \tag{3.15}$$

$$\begin{bmatrix} k_x \\ k_y \\ k_z \end{bmatrix} = \hat{\mathbf{u}}_{bend} \text{ and } v\phi = 1 - c\phi , \tag{3.16}$$

and the vectors $\mathbf{d}'_1, \mathbf{d}'_2, \mathbf{d}'_3$ represent the position of the undeflected revolutes described about the wrist center, $\mathbf{c}_W$. Thus,

$$\mathbf{d}'_i = \left[b_{i_x}, b_{i_y}, p_d\right]^T, \mathbf{c}_w = \left[0, 0, p_d\right]^T \qquad i = 1,....,3 \tag{3.17}$$

With the location of the distal revolutes known, it is possible to identify points which must lie on the plane of symmetry. Three such points may be conveniently found as follows:
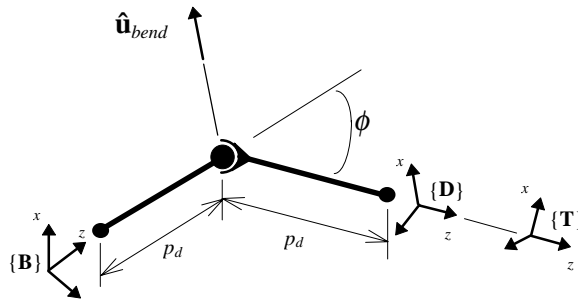

Figure 3.4: Spherical Kinematic Model

$$\mathbf{p}_i = (\mathbf{d}_i + \mathbf{b}_i)/2 \qquad i = 1,...,3 \qquad (3.18)$$

These points bisect the vector connecting the corresponding revolutes on the basal and distal plates (see Fig. 3.3). In general these points are not coincident with the midplane spheric joints, $\mathbf{m}_1$, $\mathbf{m}_2$, $\mathbf{m}_3$. Using these three bisecting points the coefficients for the equation of the midplane may be determined:

$$\mathbf{N}_m = \{A_m, B_m, C_m\}^T = (\mathbf{p}_2 - \mathbf{p}_1) \times (\mathbf{p}_3 - \mathbf{p}_1), \quad D_m = -\mathbf{N}_m \cdot \mathbf{p}_1 \qquad (3.19)$$

where $\mathbf{N}_m$ is the common normal to the midplane, and $A_m \dots D_m$ are the plane coefficients for the midplane. The basal and distal ends of the wrist are joined by three symmetric RRRRR chains. Both the basal and distal arms form circles that intersect the midplane at the location of the intersecting revolute midplane points. This is characterized in the following set of constraint equations:

$$\begin{aligned}
&|\mathbf{m}_i - \mathbf{b}_i| = l, \\
&A_c m_{i_x} + B_c m_{i_y} + C_c m_{i_z} + D_c = 0, \qquad i = 1,...,3 \qquad (3.20) \\
&A_m m_{i_x} + B_m m_{i_y} + C_m m_{i_z} + D_m = 0,
\end{aligned}$$

where $\mathbf{m}_1 \dots \mathbf{m}_3$ are the midplane nodes, l is the arm length, and $A_c \dots D_c$ represent the plane equation coefficients for the base arm circle. These three equations are solved by expanding the distance equation and substituting into each plane equation until a quadratic solution is found for each of the three nodes. Thus, the entire inverse positioning problem has eight (2^3) distinct closures.

Once each of the midplane nodes are found, the required input angles are determined as the angle between the basal arms and the unit vectors, $\hat{\mathbf{q}}_i$.

$$\theta_i = cos^{-1}\left[\frac{(\mathbf{m}_i - \mathbf{b}_i) \cdot \hat{\mathbf{q}}_i}{\|(\mathbf{m}_i - \mathbf{b}_i)\|}\right] \qquad i = 1,...,3 \qquad (3.21)$$

where θ_i, $i=1,...,3$, are the required input angles.

The final roll axis rotation may now be evaluated by observing the angle between the $\hat{\mathbf{x}}_D$ and $\hat{\mathbf{x}}_T$ axes,

$$\theta_r = \cos^{-1}\left(\hat{\mathbf{x}}_D \cdot \hat{\mathbf{x}}_T\right). \qquad (3.22)$$

For any orientation and plunge distance, it is now possible to solve for the four input angles. This solution does, however, couple the positional and orientational degrees-of-freedom and perhaps complicates the overall manipulator solution. This complication may be avoided by imposing spherical constraints which decouple the position and orientation, essentially making this a spherical wrist. Simpler, three degree-of-freedom parallel wrists have been proposed by Angeles and Gosselin (1989) and Asada and Cro Granito (1985), but these appear to lack the high dexterity and large workspace characteristics exhibited by this device

3.4 Artificially Coupled Spherical Configuration

   Imposing spherical constraints on the proposed wrist is simply a matter of specifying the plunge distance parameter, p_d, as a constant. This results in c_W, the location of the wrist's geometric center remaining fixed. In many respects, this may prove to be a useful mode in which to operate the wrist. Solutions may be generated for a six degree-of-freedom positioning problem without the need to account for the redundant plunge axis. Several two degree-of-freedom parallel pointing devices exist; for example, a single loop, spherical 5R mechanism (Ouerfelli and Kumar, 1991), and a two degree-of-freedom spherical parallel manipulator (Gosselin et. al., 1994). However, it is believed that the proposed wrist has the advantages of symmetry and a large, singularity free workspace. Additionally, it is possible that more sophisticated control methods could use this extra degree-of-freedom to optimize a given objective function, as demonstrated in Chap. 7.

3.5 Kinematic Workspace Analysis

   A kinematic workspace analysis for the new wrist concept was performed to demonstrate its range of motion. The workspace, presented in Fig. 3.5, is limited only by kinematic constraints and does not account for physical link interferences. This analysis was performed by moving the wrist model to increasingly large displacement angles and checking the kinematic position equations for closure (or assembly). In order to demonstrate the clearest visible representation, surfaces were plotted, each of which represent a different fixed plunge value, represented by the dimensionless plunge distance to leg length ratio, $R_d = p_d/l$. The available kinematic workspace is a function of the base to leg length ratio, $R_b = b/l$ and the plunge distance to leg length ratio (Canfield, Salerno, and Reinholtz, 1994). For any given R_d, the wrist sweeps through a spherically constrained workspace. To illustrate the total unconstrained kinematic wrist workspace, a series of these spherically constrained workspace plots are developed for ratios $R_d =$ 0.7467 to 0.8667, while the ratio R_b is held fixed at 0.6667. The total workspace volume may be visualized as the sum of all the individual fixed plunge ratio plots. For clarity the plots shown in Fig. 3.5 are shown separated along the vertical axis. In reality these workspace shells would be nested about a near common center.

$R_d = 0.8667$

$R_d = 0.8000$

$R_d = 0.7467$

$R_b = b/l = 0.6667$
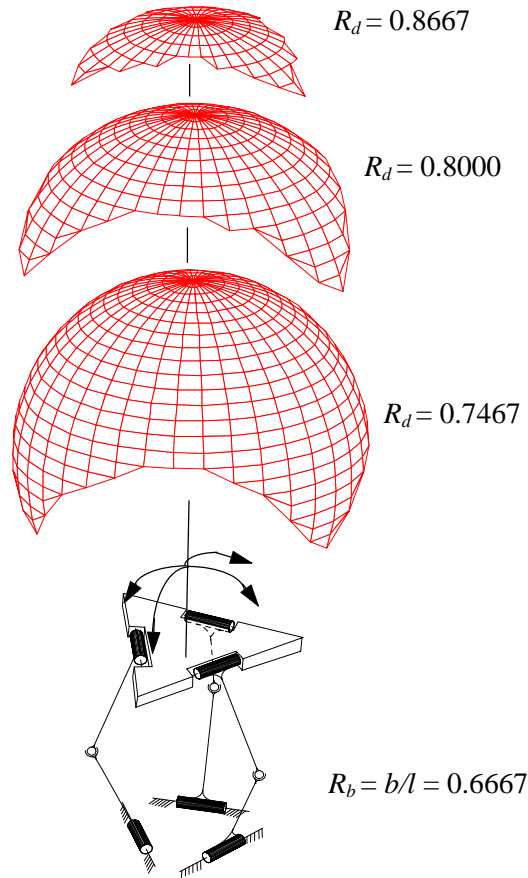
Figure 3.5: Theoretical Workspace
Corresponding to Various R_d Ratios

3.6 Conclusions to Kinematic Position Analysis

The initial position kinematic analysis of the parallel-architecture Carpal wrist concept is presented in this chapter. The geometric model and kinematic model demonstrate that the wrist possesses a number of characteristics that are beneficial and necessary to a majority of robotic manipulator applications; i.e., a large workspace, a high strength-to-weight ratio (Ganino, 1996), and an open-center architecture. The kinematic analyses result in closed-form solutions for both the forward and inverse positioning problem. The inverse kinematic problem for the wrist has been solved for the general three degree-of-freedom Wrist and the four degree-of-freedom fully orientational Wrist, providing both orientation and plunge position, and also for the constrained spherical configuration, providing only general pointing orientation. These solutions for the inverse kinematic problem are significant since they show that the Wrist may be controlled in real time with minimal computational effort. Results from the workspace analysis demonstrates the necessary large workspace for robotic wrist applications. It possesses a large, continuous workspace which can be optimized for a particular application by altering the geometric dimensions. In addition to the large workspace, the Carpal Wrist will be shown in Chap. 4 to be free of singularities within its boundaries.